Estimation of acoustic and elastic properties of plastic foam using acoustic-to-frame coupling

Ho-Chul Shin, Shahram Taherzadeh, Keith Attenborough

ACOUSTICS 2012

Estimation of acoustic and elastic properties of plastic foam using acoustic-to-frame coupling

H.-C. Shin, S. Taherzadeh and K. Attenborough

The Open University, DDEM, Maths, Computing and Technology, Walton Hall, MK7 6AA
Milton Keynes, UK
h.c.shin@open.ac.uk

Synthetic partially reticulated polyurethane foams are deployed in many situations for noise and vibration control. So understanding the behaviour of these foams when exposed to acoustic and/or mechanical waves is essential. Much progress has been made through identification and non-acoustic measurements of parameters introduced in the seminal works by Biot and, subsequently, by Allard, that describe the acoustical and elastic properties. Conversely, these parameters can be estimated from measurements of vibroacoustical responses. In principle measurements of acoustic-to-frame coupling should be more effective than measurements that focus on either acoustic or frame behaviour separately. This idea has been pursued in many papers co-authored by Walter Lauriks and Jean-François Allard. This paper describes recent demonstrations that pore-related and elastic parameters of air-saturated plastic foam can be estimated from data obtained by conjunctive use of a microphone and a laser Doppler vibrometer.

1 Introduction

Biot identified three types of elastic waves propagating in a fluid-saturated porous elastic solid: type-I and -II compressional waves and a shear wave [1]. He showed that it was possible to predict such wave propagation with a set of physical parameters which may represent a porous solid under continuum assumption. Therefore, the experimental determination of so-called Biot parameters has been an active topic since the advent of his poroelasticity theory.

For many purposes, the porous materials of interest can be considered to have rigid frames so that there is only one dominant wave type propagating inside them. The reduced number of parameters certainly helps to solve an 'inverse' problem to determine them. It has been reported [2] that tortuosity and two characteristic lengths of foams may be deduced by using a differential evolution algorithm. The measured data was normal surface impedance of a specimen fitted inside an impedance tube. The optimisation was based on the rigid-frame model of Johnson-Champoux-Allard.

Recently, to determine the rigidity parameters of reticulated foams, Biot's poroelasticity theory has been re-visited for the foams [3]. A monopole acoustic field was created above a polyurethane foam. The resulting normal and radial velocities on the foam surface were measured by a laser Doppler vibrometer (LDV). These velocities were predicted by using the Biot's poroelasticity theory and the Sommerfeld integral depicting the acoustic field of a monopole above a plane boundary. Other parameters which can be measured by resorting to a rigid-frame model were determined separately based on the measurements in a Kundt tube. Only rigidity parameters, specifically Poisson's ratio and shear modulus, were deduced by exploiting the acoustic-to-frame (A-F) coupling phenomenon.

In this paper, we have investigated the feasibility of using the A-F coupling alone to determine both the set of parameters associated with elasticity and the set usually measured using a rigid-frame model. The parameters estimated in the current work are flow resistivity, tortuosity and two independent elasticity parameters. A compression driver with an extended pipe was used to generate airborne sound, and the reflected sound and the subsequent vibration of the foam surface were recorded by a microphone and an LDV respectively. These data were used to estimate foam parameters through an inverse problem: an optimisation process minimising the differences between the data and model predictions.

2 Methods

2.1 Biot-Stoll poroelasticity model

For Biot poroelasticity theory, we need a certain number of physical parameters to describe the wave propagation within an air-saturated unbounded homogenous and isotropic poroelastic material. First set of required parameters defines the properties of interstitial air within porous frame. They are density (ρ_f), dynamic viscosity (η), atmospheric pressure (P), specific heat ratio (γ), and Prandtl number of air (N_pr). These are well documented and hence can be treated as known constants. When these are combined with a model for pore shape and structure, one can define the bulk modulus of the interstitial air (K_f):

$$K_\mathrm{f} = (\gamma P)/\left[\gamma - (\gamma - 1)H(\lambda\sqrt{N_\mathrm{pr}})\right] \tag{1}$$

Here, $H(\cdot)$ is a correction factor to account for the deviation of the interstitial air density from that of free air, and has been calculated for many ideal pore shapes [4]. The viscosity correction factor ($F(\cdot)$) for a two-dimensional pore shape was introduced in Biot's seminal paper [1]:

$$F(\lambda) = \frac{(\lambda\sqrt{-i})^2\,(1 - H(\lambda))}{3\,H(\lambda)} \tag{2}$$

$$H(\lambda) = 1 - \tanh(\lambda\sqrt{-i})/(\lambda\sqrt{-i}) \tag{3}$$

$$\lambda = \sqrt{\frac{3\rho_\mathrm{f}\,\omega\,q^2}{\Omega\,\sigma}} \tag{4}$$

,where angular frequency, tortuosity, porosity and flow resistivity are symbolised by ω, q^2, Ω and σ respectively. i is the imaginary unit of $\sqrt{-1}$ and the harmonic motion of $\exp(-i\omega t)$ is assumed with time denoted by t. There are several experimental methods to measure porosity directly. And porosity can also be calculated by invoking $\Omega = 1 - \rho_\mathrm{b}/\rho_\mathrm{s}$. The bulk density of foam (ρ_b) can be easily measured, and the density of the frame material (ρ_s) may be assumed: 1200 kg m^{-3} for polyurethane [5]. When the wavelength of interest is much larger than the typical sizes of frame and pores, the characteristic equations of the wave numbers for type-I (l_1) and -II (l_2) compressional waves and a shear wave (l_3) may be written in the Biot-Stoll formulation [6]:

$$\begin{vmatrix} H\,l_{1,2}^2 - \rho\,\omega^2 & \rho_\mathrm{f}\,\omega^2 - C\,l_{1,2}^2 \\ \rho_\mathrm{f}\,\omega^2 - C\,l_{1,2}^2 & m_\mathrm{a}\,\omega^2 - M\,l_{1,2}^2 + i\omega F\sigma \end{vmatrix} = 0\,, \tag{5}$$

$$\begin{vmatrix} \rho\,\omega^2 - \mu\,l_3^2 & \rho_{\mathrm{f}}\,\omega^2 \\ \rho_{\mathrm{f}}\,\omega^2 & m_{\mathrm{a}}\,\omega^2 + i\omega F\sigma \end{vmatrix} = 0\ . \tag{6}$$

The coefficients H, C, and M are re-formulations of the elastic constants P, Q, and R appearing in Biot's theory, and the detailed formulae can be found in Ref. [6]. m_{a} is an apparent mass defined by $q^2\rho_{\mathrm{f}}/\Omega$. And μ is the shear modulus, represented by N in Biot's original notation of P, Q, R, and N.

Since the pore-fluid related parameters are well defined for a certain idealised model for pore shape, the remaining parameters in solving the characteristic equations (Eqs. 5 and 6) are mainly frame- and structure-related. They are flow resistivity, complex bulk and shear moduli of the porous structure, and tortuosity.

2.2 Wave-propagation model

Once wave numbers of three types of elastic waves are found, the reflection and refraction of waves on layer interfaces can be determined by solving a boundary value problem. When an airborne acoustic source is placed above infinite plane interface, the resulting wave field can be considered as axisymmetric. The wave motion according to Helmholtz equation may be represented by using displacement potentials (Ψ) [7]:

$$\nabla^2\Psi_{m,n}(r,z) + l_{m,n}^2\Psi_{m,n}(r,z) = \delta_n(r,z)\ . \tag{7}$$

The second subscript n denote a layer. The first subscript m indicates the wave types: 0 for a wave in the air layer above the foam; 1 and 2 for two compressional waves, 3 for a shear wave in a foam layer. The wave number of foams (l_m for m = 1, 2, 3) are obtained by Eqs. (5) and (6). The wave number for air layer is $l_0 = \omega/c_{\mathrm{f}}$, where c_{f} is the speed of sound in air. A point source in a layer n is expressed by δ_n. Due to the nature of axisymmetric field, by applying Hankel transform, the vertical variable (z) can be separated from the radial dimension (r). The forward Hankel transform applied in the radial dimension is:

$$\psi_{m,n}(\xi,z) = \int_0^\infty \Psi_{m,n}(r,z)J_0(l_r\,r)\,r\,dr \tag{8}$$

,where $J_0(\cdot)$ is the zeroth-order Bessel functions of the first kind with a complex argument. ξ is the projection of wave number to the surface and is usually referred to as horizontal wave number. The transformed quantity ($\psi_{m,n}$) in the left-hand side is a Green's function which is dependent on depth but independent of range. Full execution of Hankel transform to Eq. (7) now leads to the following ordinary differential equation which is independent of range and is uniquely determined at a given depth (h):

$$\begin{gathered} \tfrac{d^2}{dz^2}\psi_{m,n}(\xi,h) + \beta_{m,n}^2\psi_{m,n}(\xi,h) = \delta_n(h)\ , \\ \beta_{m,n}^2 = l_{m,n}^2 - \xi^2\ . \end{gathered} \tag{9}$$

These Green's functions are built with details such as the location of a source and the amplitudes of propagating waves. For a monopole source near plane interface, the contribution from the source and the interaction with the boundary are essentially the Sommerfeld representation. And Green's functions defined at all the layers need to be calculated together by constructing a global matrix [7]. This is a system of linear equations composed of boundary conditions of all layers. For an air-foam boundary, four boundary conditions are to be met: continuity of air pressure, normal displacement, normal stress and tangential stress.

Once the Green's function is found for each layer as a function of depth of interest by Eq. (9), the displacement potentials ($\Psi_{m,n}$) at a range of interest (R) can be obtained through the inverse Hankel transform:

$$\Psi_{m,n}(R,h) = \int_0^\infty \psi_{m,n}(\xi,h)J_0(\xi\,R)\,\xi\,d\xi \tag{10}$$

Finally, the displacement potentials are converted back to particle displacements of corresponding phase, from which acoustic pressure and frame displacements are further calculated.

2.3 Measurements

For an acoustic source, we have employed a compression driver extended by a tube with an internal diameter of 2 cm. This configuration is known to be a good approximation of a monopole acoustic source in the medium audible frequency range [8]. A precision microphone (Brüel & Kjær model) has been arranged for the detection of sound field in air close to the foam surface. For the monitoring of the foam surface vibration, a laser Doppler vibrometer (Polytec model) has been deployed with the laser beam obliquely incident to the surface.

The generation and acquisition of data have been made using a National Instruments data acquisition (DAQ) board controlled by a Matlab data acquisition toolbox. A generated electrical source signal is enhanced via a power amplifier before reaching the compression driver. The detected signal by a microphone is also amplified before an analogue-to-digital converter. The laser signal is conditioned within its controller unit. Then, data from the microphone and the LDV are quantified in the DAQ board. These time-domain signals are then converted to frequency domain through discrete Fourier transform. Finally, the transfer functions of two signals are evaluated: A-F coupling for the ratio of the LDV output to a microphone signal. This transfer function is later used for deducing the foam parameters.

The heights of the microphone and the acoustic source were 28 and 154 mm. The radial distance from the source to the LDV focus and the microphone were 154 and 295 mm. The incidence angle of the laser beam was 44°. The size of polyurethane foam was 600 mm × 600 mm × 49 mm and was bonded to a medium-density fibreboard by double-side tapes.

2.4 Optimisation

An optimisation algorithm has been run to find a parameter set to minimise the difference of the measured and the simulated transfer functions (TF):

$$\sum_f \left(|\mathrm{TF}_{\mathrm{mea}}(f)| - |\mathrm{TF}_{\mathrm{sim}}(f)|\right)^2\ . \tag{11}$$

The subscripts mea and sim denote the measured and the simulated transfer functions. The simuation is carried out using the wave propagation model introduced earlier. A variable f is the temporal frequency. The difference is calculated based on the magnitudes of complex transfer functions. We have

found that the optimisation is more effective if only the magnitudes of the transfer functions are used rather than the full complex domain data. This may be because enveloping the complex data effectively smooths the measured data.

For optimisation problems, it is useful if a search space can be visualised in simulation. For a multi-dimensional optimisation, however, it is not straightforward to plot the search space of all variables in a single intuitive image. Instead, one variable (i.e., one-dimensional) or a pair of variables (i.e., two-dimensional) can be chosen at a time while the rest of variables are fixed.

Figure 1 shows the simulation of a cost function with uniformly varying flow resistivity while the rest of parameters are fixed. The simulated data for the cost function is the A-F coupling transfer function between signals from imaginary microphone and LDV. The overall shape of the cost function can be considered to be convex and well-posed. The cost function for the real part of bulk modulus of porous frame is shown in Figure 2. The search space is not as smooth as that of the flow resistivity.

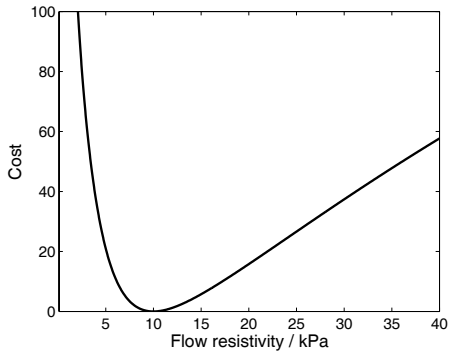

Figure 1: Simulation of a cost function of acoustic-to-frame coupling transfer function for the flow resistivity while other parameters are fixed. The exact value of the flow resistivity is 10 kPa.

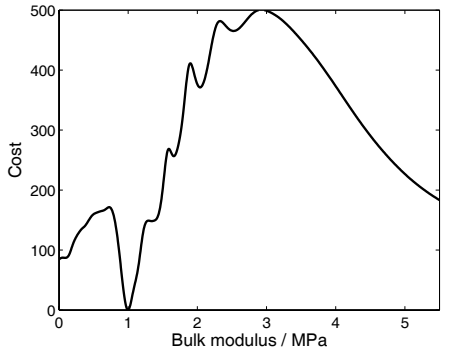

Figure 2: Simulation of a cost function of acoustic-to-frame coupling transfer function for the real part of bulk modulus while other parameters are fixed. The exact value of the modulus is 997 kPa.

When the outcomes in Figures 1 and 2 are treated as one-dimensional optimisation problems on their own, cost functions in the kind of Figure 1 can be easily addressed with a local-search algorithm, while one may need a global-search algorithm for the kind in Figure 2. When the optimisation problem is multi-dimensional, it is anticipated that the complexity of the total search space can be increased further.

As a result of the tortuous structure of the overall search space, it has been found that a single or a few executions of optimisation algorithms, regardless of local or global methods, are not up for the task addressed in this paper. An effective strategy we have found is simply to run local-search algorithms as many times as possible with different initial guesses to start the algorithm.

For the current work, we have created a Latin hypercube [9] to uniformly spread the initial guesses. For each initial seed, we have run the Rosenbrock algorithm [10] for a local search. We have then chosen the first few best solutions obtained by all local searches for further examination. Since the initial guesses are uniformly spaced by the Latin hypercube sampling, most of the search space can be assessed equally and more efficiently than by random guesses, and the chance of reaching the global solution can be increased.

3 Results

Figure 3 compares the measured A-F transfer function and the outcome of the optimisation process for polyurethane foam. The deduced parameters are:

- flow resistivity = 8760 Pa s m^{-2}
- tortuosity = 2.19
- real part of bulk modulus = 689 kPa
- real part of shear modulus = 11.5 kPa
- loss factor for both moduli = 0.09

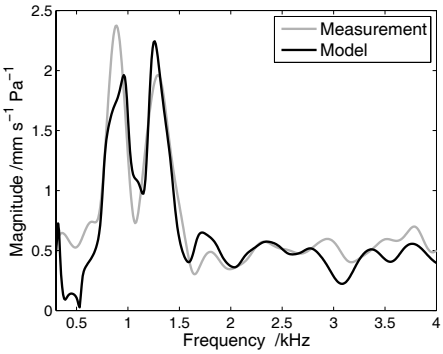

Figure 3: Comparison between the measurement and the model calculation of the acoustic-to-frame coupling over polyurethane foam.

During the optimisation, it was assumed that the loss factors for both moduli were equal. The other assumed parameters are: thickness, 49 mm; porosity, 0.98; density of polyurethane material, 1200 kg m^{-3}; air density, 1.2 kg m^{-3}; specific heat ratio for air, 1.4; Prandtl number for air, 0.71; bulk modulus for solid, 62.5 MPa; and atmospheric pressure, 101.3 kPa. The foam was assumed to be placed on a rigid acoustically impervious half-space.

4 Conclusion

A study has been made of the feasibility of deducing foam parameters using acoustic-to-frame (A-F) coupling data. A compression driver with an extended pipe was placed above

a hard-backed plastic foam layer, and the resulting acoustic field and surface particle velocity of the foam were measured by a microphone and a laser Doppler vibrometer respectively. An optimisation algorithm has been used to deduce the foam parameters by minimising the difference between the measured A-F coupling transfer function and the model calculation based on the Biot poroelasticity theory and a wave propagation model incorporating the Sommerfeld integral formulation. The deduced parameters are flow resistivity, tortuosity and two independent complex elasticity coefficients. A set of parameters has been found to produce reasonable agreement between the measured and the simulated A-F transfer functions for a partially-reticulated foam. Further work will extend the approach to a multi-layered foam.

Acknowledgments

This work was funded by the UK Engineering and Physical Sciences Research Council (grant EP/H040617/1).

References

[1] M. A. Biot. "Theory of propagation of elastic waves in a fluid-saturated porous solid. I. low-frequency range, II. higher frequency range". *Journal of the Acoustical Society of America* **28**(2), 168–191 (1956)

[2] Y. Atalla, R. Panneton. "Inverse acoustical characterization of open cell porous media using impedance tube measurements". *Canadian Acoustics* **33**(1), 11–24 (2005)

[3] J. F. Allard, B. Brouard, N. Atalla, G. Sebastian. "Excitation of soft porous frame resonances and evaluation of rigidity coefficients". *Journal of the Acoustical Society of America* **121**(1), 78–84 (2007)

[4] K. Attenborough, K. M. Li, K. Horoshenkov. *Predicting Outdoor Sound*. Taylor & Francis, London (2007)

[5] N. Kino, G. Nakano, Y. Suzuki. "Non-acoustical and acoustical properties of reticulated and partially reticulated polyurethane foams". *Applied Acoustics* **73**, 95–108 (2012)

[6] R. D. Stoll. "Acoustic waves in saturated sediments". In: L. Hampton, ed., "Physics of Sound in Marine Sediments", 19–39. Plenum Press, New York (1974)

[7] S. Tooms, S. Taherzadeh, K. Attenborough. "Sound propagation in a refracting fluid above a layered fluid-saturated porous elastic material". *Journal of the Acoustical Society of America* **93**(1), 173–181 (1993)

[8] J. F. Allard, N. Atalla. *Propagation of Sound in Porous Media: Modelling Sound Absorbing Materials*. John Wiley & Sons, Chichester, 2nd edition (2009)

[9] A. I. J. Forrester, A. Sóbester, A. J. Keane. *Engineering Design via Surrogate Modelling: A Practical Guide*. John Wiley & Sons, Chichester (2008)

[10] H. H. Rosenbrock. "An automatic method for finding the greatest or least value of a function". *Computer Journal* **3**(3), 175–184 (1960)